ACS APPLIED MATERIALS & INTERFACES

Research Article

www.acsami.org

Improvement of the Cycling Performance and Thermal Stability of Lithium-Ion Cells by Double-Layer Coating of Cathode Materials with Al_2O_3 Nanoparticles and Conductive Polymer

Yoon-Sung Lee,[†] Won-Kyung Shin,[‡] Aravindaraj G Kannan,[‡] Sang Man Koo,[‡] and Dong-Won Kim*[,‡]

[†]Center for Energy Convergence, Korea Institute of Science and Technology, Seoul 136-791, Korea

[‡]Department of Chemical Engineering, Hanyang University, Seoul 133-791, Korea

Supporting Information

ABSTRACT: We demonstrate the effectiveness of dual-layer coating of cathode active materials for improving the cycling performance and thermal stability of lithium-ion cells. Layered nickel-rich $LiNi_{0.6}Co_{0.2}Mn_{0.2}O_2$ cathode material was synthesized and double-layer coated with alumina nanoparticles and poly(3,4-ethylenedioxythiophene)-*co*-poly(ethylene glycol). The lithium-ion cells assembled with a graphite negative electrode and a double-layer-coated $LiNi_{0.6}Co_{0.2}Mn_{0.2}O_2$ positive electrode exhibited high discharge capacity, good cycling stability, and improved rate capability. The protective double layer formed on the surface of $LiNi_{0.6}Co_{0.2}Mn_{0.2}O_2$ materials effectively inhibited the dissolution of Ni, Co, and Mn metals from cathode active materials and improved thermal stability by suppressing direct contact between electrolyte solution and delithiated $Li_{1-x}Ni_{0.6}Co_{0.2}Mn_{0.2}O_2$ materials. This effective design strategy can be adopted to enhance the cycling performance and thermal stability of other layered nickel-rich cathode materials used in lithium-ion batteries.

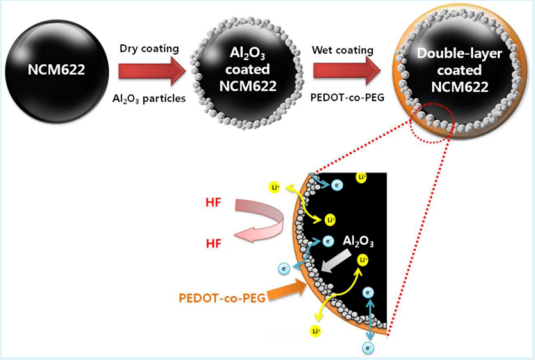

KEYWORDS: *double-layer coating, surface modification, $LiNi_{0.6}Co_{0.2}Mn_{0.2}O_2$, conductive polymer, protective coating, lithium-ion batteries*

INTRODUCTION

Significant attention has been paid to lithium-ion batteries with high energy density and long cycle life, because new applications such as electric vehicles and energy storage systems are gradually emerging onto the market.[1−7] To achieve higher energy density lithium-ion batteries, several attempts have been made to develop cathode materials with high specific capacity. As active cathode materials, nickel-rich layered $LiNi_xCo_yMn_{1-x-y}O_2$ materials have received much attention because of their high specific capacity, relatively low cost, and environmental benignancy compared to existing cathode materials.[8−18] However, their cycling stability is not good when the $LiNi_xCo_yMn_{1-x-y}O_2$ materials are cycled at high temperatures because of dissolution of transition metals from the cathode active materials and side reactions with the electrolyte solution at high voltages. Therefore, nickel-rich layered $LiNi_xCo_yMn_{1-x-y}O_2$ materials exhibit structural and thermal instabilities in the fully charged state, resulting in poor cycle stability. To solve these problems, the surfaces of cathode active materials have been coated with inorganic materials such as Al_2O_3, SiO_2, ZrO_2, TiO_2, $AlPO_4$, Li_2ZrO_3, and AlF_3.[19−29] However, these inorganic materials have low Li diffusivities and increased interfacial resistances, thereby decreasing battery performance. Conductive polymers could also be used for surface-modification of active cathode materials to enhance their cycling performance.[30−37] In our earlier study, we coated conductive poly(3,4-ethylenedioxythiophene)-*co*-poly(ethylene glycol) (PEDOT-*co*-PEG) copolymer on $LiNi_{0.6}Co_{0.2}Mn_{0.2}O_2$ (NCM) cathode material to inhibit the dissolution of transition metals from the NCM materials and suppress the electrolyte decomposition at high voltages.[36] The dual-conductive polymer that transports both Li^+ ions and electrons through the thin coating layer could lower the charge transfer resistance on the surface of NCM electrode. In light of these previous studies, we were interested in investigating the effect of modifying the surface of NCM material by double-layer coating using both inorganic particles and conductive polymer. In this work, we demonstrated that combined use of both inorganic and polymeric coatings enhanced the cycling performance and thermal stability of the NCM cathode material. Layered $LiNi_{0.6}Co_{0.2}Mn_{0.2}O_2$ cathode material was synthesized and double-layer coated with Al_2O_3 nanoparticles and conductive PEDOT-*co*-PEG copolymer. Lithium-ion cells composed of a graphite negative electrode and a surface-modified NCM positive electrode were assembled, and their cycling performances and thermal stability were evaluated. Double-layer

Received: March 30, 2015
Accepted: June 9, 2015
Published: June 17, 2015

DOI: 10.1021/acsami.5b02690
ACS Appl. Mater. Interfaces 2015, 7, 13944−13951

coating of NCM materials with Al_2O_3 and PEDOT-*co*-PEG was very effective in improving the discharge capacity, capacity retention, rate capability, and thermal stability compared to cells with pristine or single-layer coated NCM cathode materials.

EXPERIMENTAL SECTION

Double-Layer Coating of $LiNi_{0.6}Co_{0.2}Mn_{0.2}O_2$. $LiNi_{0.6}Co_{0.2}Mn_{0.2}O_2$ materials were synthesized as reported previously.[38] $[Ni_{0.6}Co_{0.2}Mn_{0.2}](OH)_2$ powder was prepared by a coprecipitation method using $NiSO_4{\cdot}6H_2O$, $CoSO_4{\cdot}7H_2O$, and $MnSO_4{\cdot}5H_2O$ as starting materials. Spherical $[Ni_{0.6}Co_{0.2}Mn_{0.2}](OH)_2$ powder was filtered, washed with deionized water, and dried at 110 °C for 24 h to remove adsorbed water. A mixture of the dehydrate $[Ni_{0.6}Co_{0.2}Mn_{0.2}](OH)_2$ and $LiOH{\cdot}H_2O$ was preheated to 480 °C for 5 h and then heated at 850 °C for 15 h under oxygen flow to obtain $LiNi_{0.6}Co_{0.2}Mn_{0.2}O_2$ materials. The $LiNi_{0.6}Co_{0.2}Mn_{0.2}O_2$ materials synthesized were double-layer coated using a two-step procedure to form a highly continuous and stable layer on the cathode surface, as illustrated in Figure 1. In the first step, aluminum oxide (Al_2O_3) powder with a particle size of 2−4 nm (Aldrich) and $LiNi_{0.6}Co_{0.2}Mn_{0.2}O_2$ materials were dry mixed at a mass ratio of 0.5:99.5 using a ball-milling machine for 4 h to obtain Al_2O_3-coated NCM material. In the subsequent step, the Al_2O_3 coated-NCM material was added to a polymer solution containing 0.5 wt % PEDOT-*co*-PEG in n-methyl pyrrolidone (NMP), and the resulting solution was stirred at 60 °C for 4 h to coat the surface of the Al_2O_3-coated NCM material with PEDOT-*co*-PEG polymer. After filtering and vacuum drying at 100 °C, double-layer coated NCM (dl-NCM) powder was finally obtained. In addition, Al_2O_3-coated NCM (al-NCM) and conductive PEDOT-*co*-PEG-coated NCM (cp-NCM) materials were prepared using a similar one-step coating process for use as control samples.

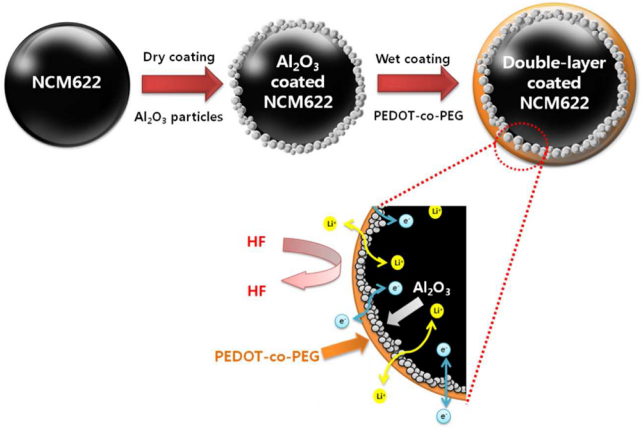

Figure 1. Schematic of double-layer coating of $LiNi_{0.6}Co_{0.2}Mn_{0.2}O_2$ material with Al_2O_3 nanoparticles and PEDOT-*co*-PEG.

Preparation of Electrodes and Cell Assembly. To prepare the positive electrode, we blended the surface-modified $LiNi_{0.6}Co_{0.2}Mn_{0.2}O_2$ powder, poly(vinylidene fluoride) (PVdF), and super-P carbon at a weight ratio of 85:7.5:7.5 in NMP solvent and the resultant slurry was coated onto an aluminum foil. Its active mass loading was controlled to have a capacity of about 1.0 mAh cm^{-2}. Similarly, the negative electrode was prepared by coating a NMP-based slurry containing mesocarbon microbead, PVdF, and super-P carbon onto a copper foil. The capacity ratio of the negative electrode to the positive electrode was about 1.15. The electrodes were vacuum-dried at 110 °C for 12 h and roll-pressed. Then the electrodes were assembled into CR2032 coin-type cells with a polypropylene separator (Celgard 2400) and liquid electrolyte (1.15 M $LiPF_6$ in EC/DEC, 3/7 by volume) in an Ar-filled glovebox.

Measurements. The morphologies of pristine and surface-modified NCM particles were examined by scanning electron microscopy (SEM, JEOL JSM-6300) and transmission electron microscopy (TEM, JEOL 2010). Energy dispersive X-ray spectroscopy (EDX) mapping was used for morphological assessment and surface elemental characterization on the surface-modified NCM particles. The electronic and ionic conductivities of the NCM materials were measured by four-point probe method and AC impedance technique, respectively, as described in previous literature.[36] Fourier transform infrared (FT-IR) measurements were performed on JASCO 460 IR spectrometer. Thermogravimetric analysis (TGA) measurements were carried at a heating rate of 5 °C min^{-1} using TGA/DSC analyzer (SDT Q600, TA Instrument). The crystalline phase of NCM powders was characterized by powder X-ray diffraction (XRD) (Rigaku, Rint-2000) using Cu Kα radiation. Charge and discharge cycling tests of the lithium-ion cells were conducted over the voltage range of 2.6−4.3 V using a battery cycler (WBCS 3000, Wonatech) at 25 and 55 °C, respectively. AC impedance measurements of the lithium-ion cells were conducted using a Zahner Electrik IM6 impedance analyzer in the frequency range of 1 mHz to 100 kHz with an AC voltage amplitude of 10 mV. The amount of Ni, Co and Mn dissolved from the charged $LiNi_{0.6}Co_{0.2}Mn_{0.2}O_2$ electrodes into the liquid electrolyte was measured by atomic absorption spectroscopy (AA, vario 6, Analyticjena). HF content measurements in the electrolyte were performed by an acid−base titration method.[39] For differential scanning calorimetry (DSC) experiments, lithium-ion cells were fully recharged to 4.3 V after 100 cycles. After disassembling the cells, the positive electrode was scraped from the aluminum current collector. Approximately 5 mg of the positive electrode was hermetically sealed in a stainless steel pan and measurements were conducted at a heating rate of 1 °C min^{-1}.

RESULTS AND DISCUSSION

The morphologies of pristine and surface-modified $LiNi_{0.6}Co_{0.2}Mn_{0.2}O_2$ particles were characterized using SEM measurements, and the results are shown in Figure S1 in the Supporting Information. The primary particles protruded slightly toward the outside of large spherical secondary particles. There is no significant difference between the pristine and surface-modified NCM particles in the SEM images. EDX mapping images of various elements in the dl-NCM were obtained to examine the distribution of elements on the surface of dl-NCM coated by Al_2O_3 and PEDOT-*co*-PEG. As shown in Figure 2, homogeneous distributions of Ni, Co and Mn in the $LiNi_{0.6}Co_{0.2}Mn_{0.2}O_2$ particles were clearly observed in the dl-NCM particles. It was also evident that aluminum and sulfur elements were evenly distributed on the surface of the dl-NCM particles, which indicated that the surface of the NCM material was uniformly coated with both Al_2O_3 nanoparticles and PEDOT-*co*-PEG polymer. The content of alumina on the surface of dl-NCM was determined to be about 0.42 wt % by EDX analysis, whereas that of PEDOT-*co*-PEG was 0.46 wt % based on thermogravimetric analysis (Figure S2 in the Supporting Information).

To confirm the uniform coating of NCM particles with Al_2O_3 nanoparticles and PEDOT-*co*-PEG, we carried out TEM measurements, and the TEM images of pristine NCM and surface-modified NCM particles are shown in Figure 3. The pristine NCM particle did not have any outer layer. In contrast, a TEM image of cp-NCM revealed that NCM particle was evenly surface-coated by a polymer layer. An image of the al-NCM particle showed that the NCM material was covered with Al_2O_3 nanoparticles, with a coating thickness range from 18 to 38 nm. For the dl-NCM particle, Al_2O_3 nanoparticles were coated on the NCM surface, and these nanoparticles were in turn covered by an additional layer of PEDOT-*co*-PEG. As

DOI: 10.1021/acsami.5b02690
ACS Appl. Mater. Interfaces 2015, 7, 13944−13951

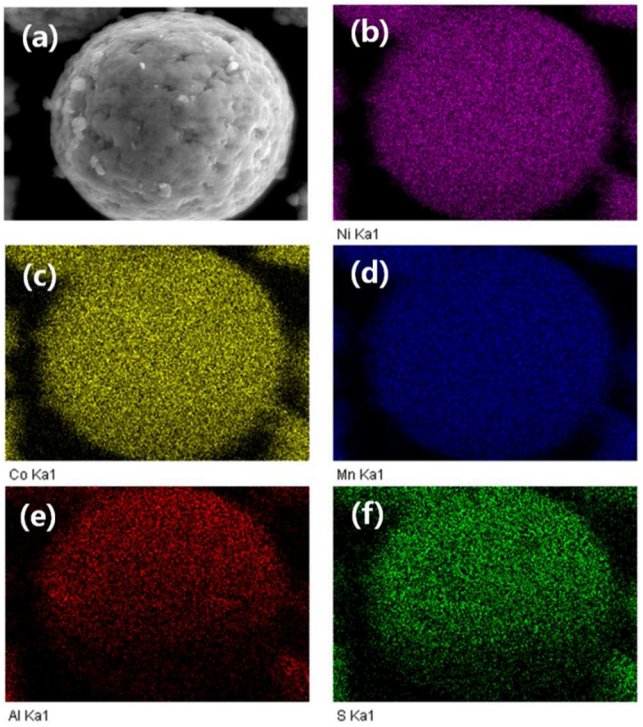

Figure 2. (a) SEM image of dl-NCM, and EDX elemental mappings corresponding to (b) Ni, (c) Co, (d) Mn, (e) Al, and (f) S in the dl-NCM.

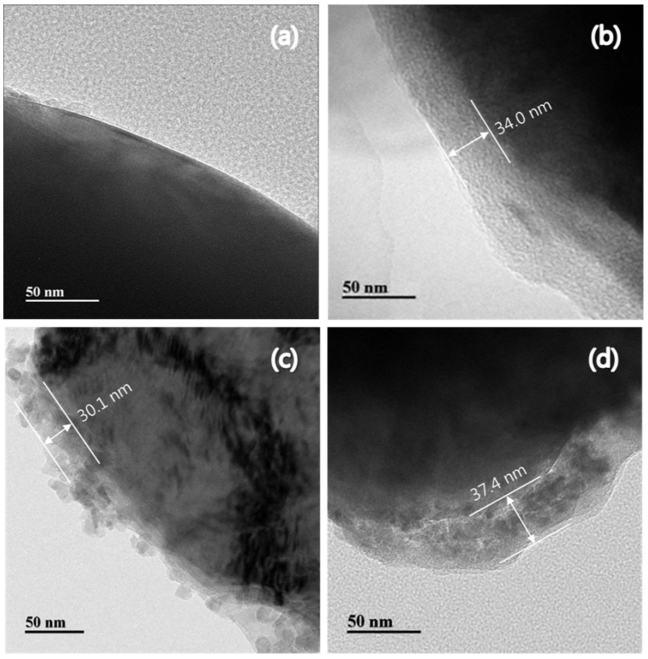

Figure 3. TEM images of (a) pristine NCM, (b) conductive polymer-coated NCM (cp-NCM), (c) alumina-coated NCM (al-NCM), and (d) double-layer-coated NCM (dl-NCM).

compared to alumina coating, which resulted in discontinuous deposition of rough surface layer, the double layer composed of Al_2O_3 and PEDOT-*co*-PEG provided highly continuous surface coverage. Figure S3 in the Supporting Information shows the selected area electron diffraction (SAED) patterns obtained from the dl-NCM particle. The SAED pattern in the left inset shows bright spot patterns, which corresponds to crystalline NCM materials. In contrast, the SAED pattern in the right inset exhibits a hollow ring pattern without bright spots, which suggests that the outer surface layer consisted of disordered polymer material. The electronic conductivities of cp-NCM and dl-NCM (1.9×10^{-1} and 1.5×10^{-1} S cm^{-1}, respectively) were much higher than those of pristine NCM (1.5×10^{-6} S cm^{-1}) and al-NCM (1.0×10^{-6} S cm^{-1}) because of the presence of conductive polymer in the coating layer. The ionic conductivity of double layer composed of Al_2O_3 and PEDOT-*co*-PEG after soaking with the liquid electrolyte was 9.5×10^{-4} S cm^{-1}, indicating facile ion transport through the thin double-layer.

The existence of PEDOT-*co*-PEG on $LiNi_{0.6}Co_{0.2}Mn_{0.2}O_2$ particle was also confirmed by the FT-IR analysis (Figure S4 in the Supporting Information). For the pristine NCM, the broad band corresponding to the M-O vibration appeared at about 540 cm^{-1}.[40] Both cp-NCM and dl-NCM exhibit the C═C ring and C−O−R vibration around 1120 cm^{-1} and C−O−C stretching vibration at 1057 cm^{-1},[34,41] confirming the presence of PEDOT-*co*-PEG in the coating layer. Figure S5 in the Supporting Information compares the XRD patterns of pristine and surface-modified NCM powders. The XRD patterns could be indexed to hexagonal a-$NaFeO_2$ structure with *R*3*m* space group without any impurity phases. No significant differences were observed in the diffraction patterns of pristine NCM and surface-modified NCM powders, indicating that surface modification of NCM powders with Al_2O_3 or/and PEDOT-*co*-PEG did not influence the crystal structure of NCM powder.

The surface-modified NCM materials were used to assemble the lithium-ion cells. The assembled cells were initially subjected to preconditioning cycles at 0.1C rate. After two preconditioning cycles, the cells were cycled in the voltage range of 2.6−4.3 V at a 0.5 *C* rate. Figure 4a shows the charge and discharge curves of a lithium-ion cell assembled with dl-NCM electrode at 0.5 *C*. The cell initially delivered a discharge capacity of 170.1 mA h g^{-1} based on $LiNi_{0.6}Co_{0.2}Mn_{0.2}O_2$ active material. After 100 cycles, the discharge capacity was slightly decreased to 163.3 mA h g^{-1}, which corresponds to 96.0% of the initial discharge capacity. Coulombic efficiency steadily increased with cycling, and it was maintained at >99.8% throughout cycling after stabilizing. Figure 4b shows the discharge capacities as a function of cycle number in the lithium-ion cells assembled with pristine NCM and surface-modified NCM electrodes. The initial discharge capacity was dependent on the type of positive electrode. The cell with al-NCM electrode showed a slightly lower initial discharge capacity (167.0 mA h g^{-1}) than the cell with pristine NCM electrode (168.3 mA h g^{-1}). This result can be ascribed to the increase of interfacial resistances due to the sluggish diffusion of Li^+ ions through an alumina coating layer, because alumina is an insulator in nature. In contrast, cells with cp-NCM and dl-NCM electrodes exhibited higher discharge capacities (171.3 and 170.1 mA h g^{-1}, respectively) than the cell with pristine NCM cathode material. We expected the conductive PEDOT-*co*-PEG polymer in the coating layer to facilitate electron transport in the cp-NCM and dl-NCM electrode. As previously reported,[42] PEDOT could also provide additional capacity as an active material. Accordingly, the cells assembled with cp-NCM and dl-NCM exhibited higher discharge capacities than cell assembled with al-NCM or pristine NCM. The capacity retention of lithium-ion cells was improved when surface-modified NCM electrodes were used rather than pristine electrode. The capacity retentions of cells with al-NCM, cp-NCM, and dl-NCM were 92.8, 93.5, and 96.0% after 100 cycles,

DOI: 10.1021/acsami.5b02690
ACS Appl. Mater. Interfaces 2015, 7, 13944−13951

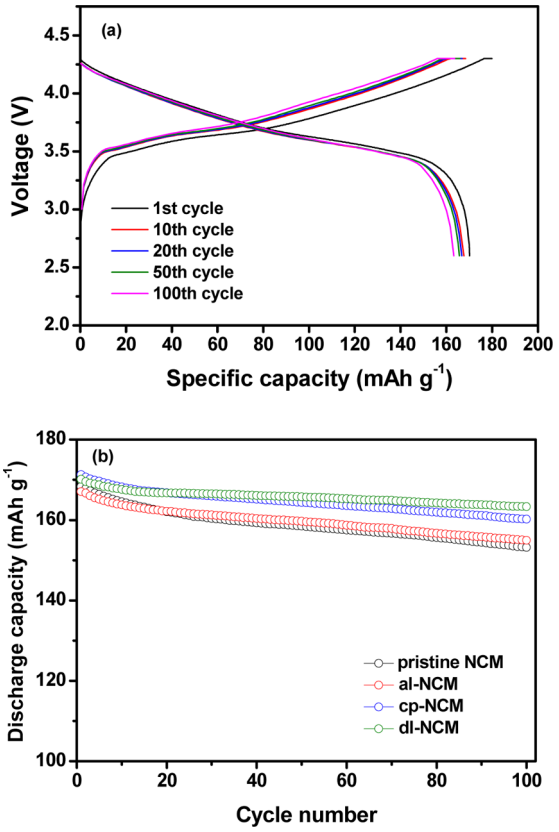

Figure 4. (a) Voltage profiles of the lithium-ion cell assembled with dl-NCM electrode (0.5 *C* constant current (CC) and constant voltage (CV) charge, 0.5 *C* CC discharge, cutoff voltage: 2.6–4.3 V), and (b) discharge capacities of lithium-ion cells assembled with pristine NCM and surface-modified NCM electrodes.

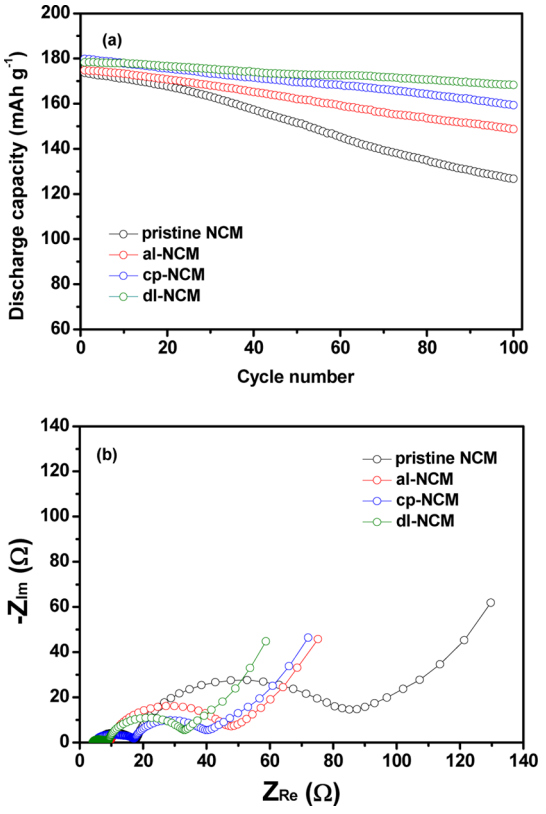

Figure 5. (a) Cycling characteristics of lithium-ion cells with pristine and surface-modified NCM materials at 55 °C and 0.5C rate, and (b) complex impedance plots of the lithium-ion cells assembled with different electrodes, which were obtained after 100 cycles at 55 °C and 0.5 *C* rate. All impedance data were obtained at 4.3 V.

whereas the cell with pristine NCM had a capacity retention of 91.0%. We ascribed the good cycling stability of the cells with surface-modified NCM electrodes to the presence of a coating layer that functioned as a protective layer to cover the NCM materials and suppress the electrolyte decomposition during cycling. It should be noted that the cell assembled with dl-NCM material exhibited better capacity retention than any of the other cells evaluated. This result suggested that the presence of an alumina layer along with a conductive polymer layer on NCM was effective at maintaining cycling stability. In particular, the flexibility of PEG can buffer the volume changes of the electrode during charge–discharge cycles,[43] resulting in better capacity retention. Figure S6 in the Supporting Information shows the TEM image of dl-NCM powder after 100 cycles, illustrating that the coating layer composed of Al_2O_3 and PEDOT-*co*-PEG is not detached from the surface of NCM particle after cycling. This result indicates that the coating layer on NCM is firmly adhesive and physically stable.

To further demonstrate the effectiveness of the double-layer coating for improving the cycling stability, we cycled the cells with pristine NCM and surface-modified NCMs at 55 °C to accelerate capacity fading. Figure 5a shows the cycling characteristics of lithium-ion cells assembled with pristine and surface-modified NCM cathode materials, which were measured at 55 °C and a 0.5 *C* rate. Overall, the initial capacities of all cells tested at 55 °C were higher than those obtained at 25 °C, which can be ascribed to the faster charge transfer kinetics at the elevated temperature. It can be clearly seen that the cycling stability was significantly improved by double-layer coating the NCM with Al_2O_3 and PEDOT-*co*-PEG. Even under these harsh test conditions, the cell with the dl-NCM electrode retained 94.3% of its initial discharge capacity after 100 cycles, whereas the capacity retention of cells with pristine NCM, al-NCM, and cp-NCM were 73.0, 85.1, and 88.6% after 100 cycles, respectively. It is well-known that layered $Li-Ni_xCo_yMn_{1-x-y}O_2$ materials exhibit large capacity decline at high temperatures due to the dissolution of transition metals from the cathode material caused by HF attack.[44] HF is known to be produced by thermal decomposition and hydrolysis of $LiPF_6$ at high temperature.[45,46] As demonstrated in Figure 1, the protective double-layer formed on the active $Li-Ni_{0.6}Co_{0.2}Mn_{0.2}O_2$ material rendered the NCM material more resistant to HF attack, and thus suppressed the dissolution of transition metals from the NCM materials into the liquid electrolyte. Moreover, Al_2O_3 particles can act as HF scavengers to maintain the structural stability of the NCM material.[47,48] In addition, PEG in the PEDOT-*co*-PEG copolymer is a Lewis base, and thus can effectively complex with thermally decomposed PF_5 that is a Lewis acid, thereby preventing its hydrolysis to produce HF. Li et al. reported that the addition of Lewis basic additives stabilized liquid electrolytes against thermal decomposition initiated by Lewis acids.[49] Consequently, the use of both Al_2O_3 particles and PEDOT-*co*-PEG in the double-layer coating could reduce the HF content in the electrolyte. To confirm this presumption, HF contents in the cells were measured after storing the cells at 55 °C for 3 days; the results are shown in Figure S7 in the Supporting

DOI: 10.1021/acsami.5b02690
ACS Appl. Mater. Interfaces 2015, 7, 13944–13951

Information. HF content decreased when surface-modified NCM electrodes were employed, and double-layer coating proved to be most effective for reducing HF content. To understand the effect of surface modification on cycling behavior at high temperature, the AC impedance of the cells was measured after the repeated cycles at 55 °C. As shown in Figure 5b, two overlapped semicircles were observed due to different contributions of interfacial resistances. According to previous studies,[50,51] the semicircle at high to middle frequency represents the resistance of the surface film (R_f), whereas the semicircle at middle to low frequency is attributed to charge transfer resistance at the electrode−electrolyte interface (R_{ct}). The cells assembled with surface-modified NCM materials exhibited much lower interfacial resistances than the cell with pristine NCM. This supported the notion that the protective layer on the NCM active particles reduced degradation of the active material by preventing its direct contact with the electrolyte during cycling at high temperature. Moreover, a highly conductive polymer in the coating layer formed on cp-NCM and dl-NCM would facilitate the electron transfer between less conductive $LiNi_{0.6}Co_{0.2}Mn_{0.2}O_2$ particles in the positive electrodes.

To confirm that the coating layers formed on the NCM material suppressed the dissolution of transition metals, we measured the contents of Ni, Co, and Mn dissolved from the pristine and surface-modified NCM materials into the electrolyte solution after the electrodes were stored for 4 weeks at 55 °C. As shown in Figure 6, the dissolved amounts of transition metals gradually increased with time for all electrodes. As discussed previously, the dissolution of transition metals is caused by HF attack, which results in capacity decline at high temperatures.[52,53] The pristine NCM electrode showed the highest amount of dissolution of Ni, Co, and Mn after 4 weeks, whereas less metals dissolved from the surface-modified NCM electrodes. Note that the lowest amount of metal dissolved in the liquid electrolyte containing dl-NCM. For dl-NCM electrode, the surface of the NCM materials was fully and densely covered by a double-layer of alumina nanoparticles and PEDOT-*co*-PEG polymer, which inhibited direct contact between the electrolyte solution and NCM materials, and effectively suppressed the dissolution of transition metals due to HF attack.

Figure 7 compares the discharge capacities of the lithium-ion cells assembled with different NCM materials, with the *C* rate increasing from 0.1 to 5.0 *C* every five cycles. Relative capacity was defined as the ratio of the discharge capacity at a specific *C* rate to the discharge capacity at a 0.1 *C* rate. Relative capacities decreased with increasing the *C* rate due to the polarization. The effect of surface modification on the rate performance of cells was noticeable as the current density was increased to 5.0 mA cm^{-2} (5.0 *C* rate). Single-layer coating with PEDOT-*co*-PEG resulted in the best high rate performance at higher *C* rates. Surface modification of NCM with conductive PEDOT-*co*-PEG polymer improved its electronic conductivity, which facilitated the electron transport. The presence of highly ion-conductive PEG in the PEDOT-*co*-PEG copolymer likely also enhanced the lithium ions transport, which is a prerequisite for a fast charge-transfer reaction. In contrast, surface coating of NCM with Al_2O_3 particles reduced the discharge capacities at high current rates, indicating that the presence of an alumina layer on the surface of NCM adversely affected the rate performance of the cell.

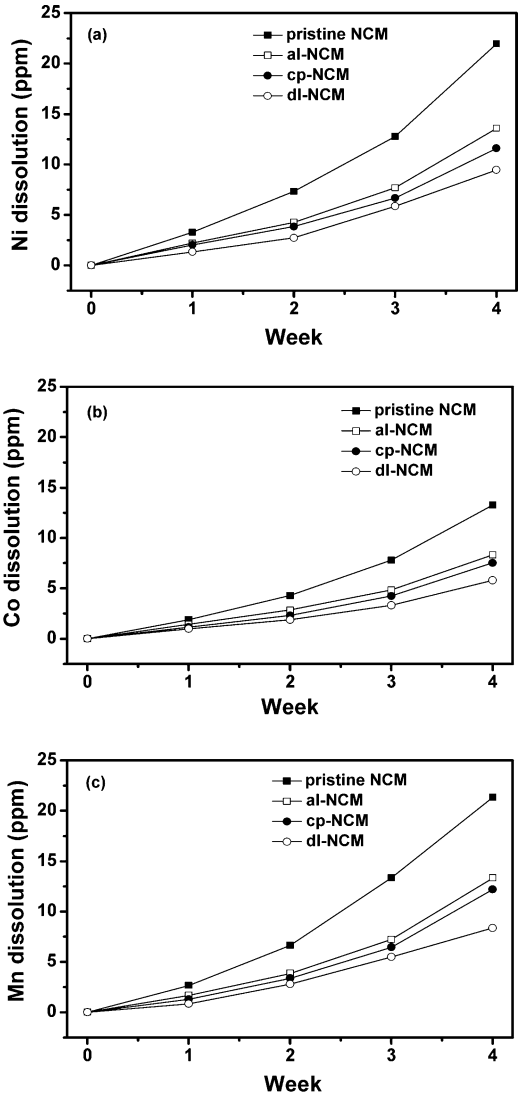

Figure 6. Amount of transition metals dissolved from the charged $LiNi_{0.6}Co_{0.2}Mn_{0.2}O_2$ electrodes into electrolyte solution at 55 °C. (a) Ni, (b) Co, and (c) Mn.

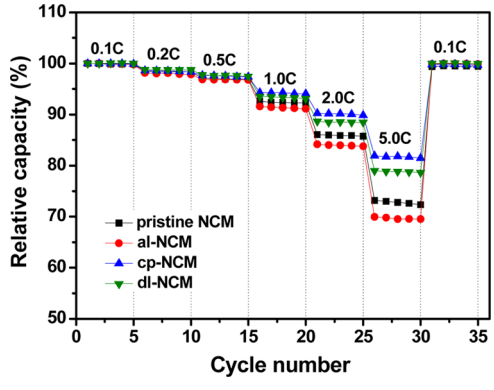

Figure 7. Rate capability of lithium-ion cells assembled with different NCM electrodes as a function of *C* rate.

The thermal stability of NCM materials in the charged state is critical for battery safety, and the thermal stability studies were performed using DSC measurements of the delithiated NCM materials ($Li_{1-x}Ni_{0.6}Co_{0.2}Mn_{0.2}O_2$). Figure 8 shows the DSC thermograms of pristine and surface-modified NCM

DOI: 10.1021/acsami.5b02690
ACS Appl. Mater. Interfaces 2015, 7, 13944−13951

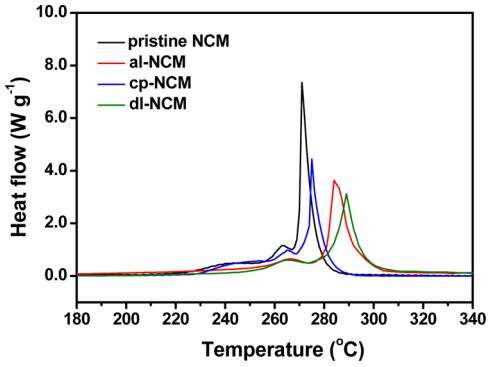

Figure 8. DSC thermograms of delithiated NCM materials charged to 4.3 V after 100 repeated cycles.

electrodes charged to 4.3 V, which are obtained after 100 cycles. The pristine NCM electrode had a main exothermic peak with a reaction heat of 601.9 J g^{-1} at 271.0 °C. In contrast, the main exothermic peaks of al-NCM and dl-NCM were shifted to 284.0 and 288.5 °C, and the heat generations were remarkably decreased to 391.0 and 345.1 J g^{-1}, respectively. This result implies that the coating layer on NCM materials reduced direct contact between the electrolyte solution and the highly unstable oxidized NCM materials, thereby rendering the cathode materials less reactive toward the liquid electrolyte. In addition, the coating layer formed on NCM material can block oxygen release from the $Li_{1-x}Ni_{0.6}Co_{0.2}Mn_{0.2}O_2$ cathode particles and in turn shifted the exothermic oxidation reaction to a higher temperature as well as reduced heat generation. However, the improvement in thermal stability of the cell with the cp-NCM electrode was not significant, indicating that incorporation of Al_2O_3 particles into the coating layer is important for enhancing the thermal stability of cathode materials due to the inherently high thermal stability of ceramic particles. Our results clearly show that double-layer coating of NCM materials with Al_2O_3 nanoparticles and PEDOT-*co*-PEG was very effective for improving their thermal stability as well as cycling performance compared to cells with pristine or single-layer coated NCM cathode materials.

CONCLUSIONS

We synthesized layered $LiNi_{0.6}Co_{0.2}Mn_{0.2}O_2$ materials, and then surface modified these materials with nanosized alumina particles and conductive PEDOT-*co*-PEG copolymer. Lithium-ion cells assembled with double-layer-coated NCM cathode materials delivered a high discharge capacity and showed better capacity retention than cells with pristine NCM materials or single-layer-coated NCM materials. Presence of a double layer on the NCM materials enhanced the cycling stability of the Li-ion cell by suppressing the dissolution of transition metals from the NCM material due to HF attack. The double-layer coating of NCM materials rendered the electrodes less reactive toward the liquid electrolyte at high temperatures, thereby improving their thermal stability. This effective strategy could be extended to other cathode materials to obtain lithium-ion batteries with enhanced safety and good cycling stability.

ASSOCIATED CONTENT

Supporting Information

SEM images of pristine and surface-modified NCM materials. TGA plot and EDX spectrum of dl-NCM. SAED patterns of dl-NCM. FT-IR spectra of pristine NCM, PEDOT-*co*-PEG, cp-NCM and dl-NCM. XRD patterns of pristine and surface-modified NCM powders. TEM image of dl-NCM after cycling. HF contents in cells assembled with pristine and surface-modified NCM electrodes. The Supporting Information is available free of charge on the ACS Publications website at DOI: 10.1021/acsami.5b02690.

AUTHOR INFORMATION

Corresponding Author

*E-mail: dongwonkim@hanyang.ac.kr.

Notes

The authors declare no competing financial interest.

ACKNOWLEDGMENTS

This work was supported by the Basic Science Research Program of the National Research Foundation of Korea (NRF), funded by the Ministry of Science, ICT and Future Planning (2014R1A2A2A01002154), and by a grant from the Human Resources Development Program of KETEP, funded by the Ministry of Trade, Industry and Energy of Korea (No. 20124010203290).

REFERENCES

(1) Tarascon, J. M.; Armand, M. Issues and Challenges Facing Rechargeable Lithium Batteries. *Nature* **2001**, *414*, 359−367.
(2) Armand, M.; Tarascon, J. M. Building Better Batteries. *Nature* **2008**, *451*, 652−657.
(3) Bruce, P. G.; Scrosati, B.; Tarascon, J. M. Nanomaterials for Rechargeable Lithium Batteries. *Angew. Chem., Int. Ed.* **2008**, *47*, 2930−2946.
(4) Etacheri, V.; Marom, R.; Elazari, R.; Salitra, G.; Aurbach, D. Challenges in the Development of Advanced Li-Ion Batteries: A Review. *Energy Environ. Sci.* **2011**, *4*, 3243−3262.
(5) Yang, Z.; Zhang, J.; Kintner-Meyer, M. C. W.; Lu, X.; Choi, D.; Lemmon, J. P.; Liu, J. Electrochemical Energy Storage for Green Grid. *Chem. Rev.* **2011**, *111*, 3577−3613.
(6) Marom, R.; Amalraj, S. F.; Leifer, N.; Jacob, D.; Aurbach, D. A Review of Advanced and Practical Lithium Battery Materials. *J. Mater. Chem.* **2011**, *21*, 9938−9954.
(7) Goodenough, J. B.; Park, K. S. The Li-Ion Rechargeable Battery: A Perspective. *J. Am. Chem. Soc.* **2013**, *135*, 1167−1176.
(8) Venkatraman, S.; Choi, J.; Manthiram, A. Factors Influencing the Chemical Lithium Extraction Rate from Layered $LiNi_{1-y-z}Co_yMn_zO_2$ Cathodes. *Electrochem. Commun.* **2004**, *6*, 832−837.
(9) Sun, Y. K.; Kim, D. H.; Jung, H. G.; Myung, S. T.; Amine, K. High-Voltage Performance of Concentration-Gradient Li-$[Ni_{0.67}Co_{0.15}Mn_{0.18}]O_2$ Cathode Material for Lithium-Ion Batteries. *Electrochim. Acta* **2010**, *55*, 8621−8627.
(10) Li, Z.; Chernova, N. A.; Roppolo, M.; Upreti, S.; Petersburg, C.; Alamgir, F. M.; Whittingham, M. S. Comparative Study of the Capacity and Rate Capability of $LiNi_yMn_yCo_{1-2y}O_2$ (y = 0.5, 0.45, 0.4, 0.33). *J. Electrochem. Soc.* **2011**, *158*, A516−A522.
(11) Xiong, X.; Wang, Z.; Huang, B.; Zhang, Q.; Li, X. Enhanced Eelectrochemical Properties of Lithium-Reactive V_2O_5 Coated on the $LiNi_{0.8}Co_{0.1}Mn_{0.1}O_2$ Cathode Material for Lithium Ion Batteries at 60 °C. *J. Mater. Chem. A* **2013**, *1*, 1284−1288.
(12) Xiong, X.; Wang, Z.; Yan, G.; Guo, H.; Li, X. Role of V_2O_5 Coating on $LiNiO_2$-Based Materials for Lithium Ion Battery. *J. Power Sources* **2014**, *245*, 183−193.
(13) Xiong, X.; Ding, D.; Bu, Y.; Wang, Z.; Huang, B.; Guo, H.; Li, X. Enhanced Electrochemical Properties of a $LiNiO_2$-Based Cathode Material by Removing Lithium Residues with $(NH_4)_2HPO_4$. *J. Mater. Chem. A* **2014**, *2*, 11691−11696.
(14) Huang, B.; Li, X.; Wang, Z.; Guo, H.; Shen, L.; Wang, J. A Comprehensive Study on Electrochemical Performance of Mn-

Surface-Modified $LiNi_{0.8}Co_{0.15}Al_{0.05}O_2$ Synthesized by an In Situ Oxidizing-Coating Method. *J. Power Sources* **2014**, *252*, 200−207.
(15) Liu, W.; Oh, P.; Liu, X.; Lee, M. J.; Cho, W.; Chae, S.; Kim, Y.; Cho, J. Nickel-Rich Layered Lithium Transition-Metal Oxide for High-Energy Lithium-Ion Batteries. *Angew. Chem., Int. Ed.* **2015**, *54*, 4440−4457.
(16) Zheng, J.; Kan, W. H.; Manthiram, A. Role of Mn Content on the Electrochemical Properties of Nickel-Rich Layered $LiNi_{0.8-x}Co_{0.1}Mn_{0.1+x}O_2$ ($0.0 \leq x \leq 0.08$) Cathodes for Lithium-Ion Batteries. *ACS Appl. Mater. Interfaces* **2015**, *7*, 6926−6934.
(17) Wu, F.; Tian, J.; Su, Y.; Wang, J.; Zhang, C.; Bao, L.; He, T.; Li, J.; Chen, S. Effect of Ni^{2+} Content on Lithium/Nickel Disorder for Ni-Rich Cathode Materials. *ACS Appl. Mater. Interfaces* **2015**, *7*, 7702−7708.
(18) Wang, D.; Li, X.; Wang, W.; Wang, Z.; Guo, H.; Ru, J. Improvement of High Voltage Electrochemical Performance of $LiNi_{0.5}Co_{0.2}Mn_{0.3}O_2$ Cathode Materials via Li_2ZrO_3 Coating. *Ceram. Int.* **2015**, *41*, 6663−6667.
(19) Cho, J.; Kim, Y.; Kim, Y.; Park, B. Zero-Strain Intercalation Cathode for Rechargeable Li-Ion Cell. *Angew. Chem., Int. Ed.* **2001**, *40*, 3367−3369.
(20) Omanda, H.; Brousse, T.; Marhic, C.; Schleich, D. M. Improvement of the Thermal Stability of $LiNi_{0.8}Co_{0.2}O_2$ Cathode by a SiO_x Protective Coating. *J. Electrochem. Soc.* **2004**, *151*, A922−A929.
(21) Fan, Y.; Wang, J.; Tang, Z.; He, W.; Zhang, J. Effects of the Nanostructured SiO_2 Coating on the Performance of $LiNi_{0.5}Mn_{1.5}O_4$ Cathode Materials for High-Voltage Li-Ion Batteries. *Electrochim. Acta* **2007**, *52*, 3870−3875.
(22) Chen, Z.; Qin, Y.; Amine, K.; Sun, Y. K. Role of Surface Coating on Cathode Materials for Lithium-Ion Batteries. *J. Mater. Chem.* **2010**, *20*, 7606−7612.
(23) Myung, S. T.; Amine, K.; Sun, Y. K. Surface Modification of Cathode Materials from Nano- to Microscale for Rechargeable Lithium-Ion Batteries. *J. Mater. Chem.* **2010**, *20*, 7074−7095.
(24) Chen, Y.; Zhang, Y.; Chen, B.; Wang, Z.; Lu, C. An Approach to Application for $LiNi_{0.6}Co_{0.2}Mn_{0.2}O_2$ Cathode Material at High Cutoff Voltage by TiO_2 Coating. *J. Power Sources* **2014**, *256*, 20−27.
(25) Cho, W.; Kim, S. M.; Song, J. H.; Yim, T.; Woo, S. G.; Lee, K. W.; Kim, J. S.; Kim, Y. J. Improved Electrochemical and Thermal Properties of Nickel Rich $LiNi_{0.6}Co_{0.2}Mn_{0.2}O_2$ Cathode Materials by SiO_2 Coating. *J. Power Sources* **2015**, *282*, 45−50.
(26) Mauger, A.; Julien, C. Surface Modifications of Electrode Materials for Lithium-Ion Batteries: Status and Trends. *Ionics* **2014**, *20*, 751−787.
(27) Liao, J.−Y.; Manthiram, A. Surface-Modified Concentration-Gradient Ni-Rich Layered Oxide Cathodes for High-Energy Lithium-Ion Batteries. *J. Power Sources* **2015**, *282*, 429−436.
(28) Zhang, X.; Sun, S.; Wu, Q.; Wan, N.; Pan, D.; Bai, Y. Improved Electrochemical and Thermal Performances of Layered $Li[Li_{0.2}Ni_{0.17}Co_{0.07}Mn_{0.56}]O_2$ via Li_2ZrO_3 Surface Modification. *J. Power Sources* **2015**, *282*, 378−384.
(29) Wu, F.; Zhang, X.; Zhao, T.; Li, L.; Xie, M.; Chen, R. Multifunctional $AlPO_4$ Coating for Improving Electrochemical Properties of Low-Cost $Li[Li_{0.2}Fe_{0.1}Ni_{0.15}Mn_{0.55}]O_2$ Cathode Materials for Lithium-Ion Batteries. *ACS Appl. Mater. Interfaces* **2015**, *7*, 3773−3781.
(30) Arbizzani, C.; Balducci, A.; Mastragostino, M.; Rossi, M.; Soavi, F. $Li_{1.01}Mn_{1.97}O_4$ Surface Modification by Poly(3,4-ethylenedioxythiophene). *J. Power Sources* **2003**, *119−121*, 695−700.
(31) Park, K.-S.; Schougaard, S. B.; Goodenough, J. B. Conducting-Polymer/Iron-Redox-Couple Composite Cathodes for Lithium Secondary Batteries. *Adv. Mater.* **2007**, *19*, 848−851.
(32) Lee, K. S.; Sun, Y. K.; Noh, J.; Song, K. S.; Kim, D. W. Improvement of High Voltage Cycling Performance and Thermal Stability of Lithium−Ion Cells by Use of a Thiophene Additive. *Electrochem. Commun.* **2009**, *11*, 1900−1903.
(33) Fedorkova, A.; Orinakova, R.; Orinak, A.; Talian, I.; Heile, A.; Wiemhofer, H. D.; Kaniansky, D.; Arlinghaus, H. F. PPy Doped PEG Conducting Polymer Films Synthesized on $LiFePO_4$ Particles. *J. Power Sources* **2010**, *195*, 3907−3912.
(34) Lepage, D.; Michot, C.; Liang, G.; Gauthier, M.; Schougaard, S. B. A Soft Chemistry Approach to Coating of $LiFePO_4$ with a Conducting Polymer. *Angew. Chem., Int. Ed.* **2011**, *50*, 6884−6887.
(35) Lee, Y. S.; Lee, K. S.; Sun, Y. K.; Lee, Y. M.; Kim, D. W. Effect of an Organic Additive on the Cycling Performance and Thermal Stability of Lithium-Ion Cells Assembled with Carbon Anode and $LiNi_{1/3}Co_{1/3}Mn_{1/3}O_2$ Cathode. *J. Power Sources* **2011**, *196*, 6997−7001.
(36) Ju, S. H.; Kang, I. S.; Lee, Y. S.; Shin, W. K.; Kim, S.; Shin, K.; Kim, D. W. Improvement of the Cycling Performance of $LiNi_{0.6}Co_{0.2}Mn_{0.2}O_2$ Cathode Active Materials by a Dual-Conductive Polymer Coating. *ACS Appl. Mater. Interfaces* **2014**, *6*, 2546−2552.
(37) Lee, J.; Choi, W. Surface Modification of Over-Lithiated Layered Oxides with PEDOT:PSS Conducting Polymer in Lithium-Ion Batteries. *J. Electrochem. Soc.* **2015**, *162*, A743−A748.
(38) Woo, S. U.; Yoon, C. S.; Amine, K.; Belharouak, I.; Sun, Y. K. Significant Improvement of Electrochemical Performance of AlF_3-Coated $Li[Ni_{0.8}Co_{0.1}Mn_{0.1}]O_2$ Cathode Materials. *J. Electrochem. Soc.* **2007**, *154*, A1005−A1009.
(39) Sun, Y. K.; Hong, K. J.; Prakash, J.; Amine, K. Electrochemical Performance of Nano-Sized ZnO-Coated $LiNi_{0.5}Mn_{1.5}O_4$ Spinel as 5 V Materials at Elevated Temperatures. *Electrochem. Commun.* **2002**, *4*, 344−348.
(40) Liu, X.; Li, H.; Li, D.; Ishida, M.; Zhou, H. PEDOT Modified $LiNi_{1/3}Co_{1/3}Mn_{1/3}O_2$ with Enhanced Electrochemical Performance for Lithium Ion Batteries. *J. Power Sources* **2013**, *243*, 374−380.
(41) Tang, Z.; Wang, J.; Chen, Q.; He, W.; Shen, C.; Mao, X.-X.; Zhang, J. A Novel PEO-Based Composite Polymer Electrolyte with Absorptive Glass Mat for Li-Ion Batteries. *Electrochim. Acta* **2007**, *52*, 6638−6643.
(42) Zhan, L.; Song, Z.; Zhang, J.; Tang, J.; Zhan, H.; Zhou, Y.; Zhan, C. PEDOT: Cathode Active Material with High Specific Capacity in Novel Electrolyte System. *Electrochim. Acta* **2008**, *53*, 8319−8323.
(43) Fedorkova, A.; Orinakova, R.; Orinak, A.; Wiemhofer, H. D.; Kaniansky, D.; Winter, M. M. Surface Treatment of $LiFePO_4$ Cathode Material with PPy/PEG Conductive Layer. *J. Solid State Electrochem.* **2010**, *14*, 2173−2178.
(44) Woo, S. U.; Park, B. C.; Yoon, C. S.; Myung, S. T.; Prakash, J.; Sun, Y. K. Improvement of Electrochemical Performances of $Li[Ni_{0.8}Co_{0.1}Mn_{0.1}]O_2$ Cathode Materials by Fluorine Substitution. *J. Electrochem. Soc.* **2007**, *154*, A649−A655.
(45) Zinigrad, E.; Larush-Asraf, L.; Gnanaraj, J.S.; Sprecher, M.; Aurbach, D. On the Thermal Stability of $LiPF_6$. *Thermochim. Acta* **2005**, *438*, 184−191.
(46) Yang, H.; Zhuang, G. V.; Ross, P. N., Jr. Thermal Stability of $LiPF_6$ Salt and Li-Ion Battery Electrolytes Containing $LiPF_6$. *J. Power Sources* **2006**, *161*, 573−579.
(47) Liu, L.; Wang, Z.; Li, H.; Chen, L.; Huang, X. Al_2O_3-Coated $LiCoO_2$ as Cathode Material for Lithium Ion Batteries. *Solid State Ionics* **2002**, *152−153*, 341−346.
(48) Myung, S.-T.; Izumi, K.; Komaba, S.; Sun, Y.-K.; Yashiro, H.; Kumagai, N. Role of Alumina Coating on Li−Ni−Co−Mn−O Particles as Positive Electrode Material for Lithium-Ion Batteries. *Chem. Mater.* **2005**, *17*, 3695−3704.
(49) Li, W.; Campion, C.; Lucht, B. L.; Ravdel, B.; DiCarlo, J.; Abraham, K. M. Additives for Stabilizing $LiPF_6$-Based Electrolytes Against Thermal Decomposition. *J. Electrochem. Soc.* **2005**, *152*, A1361−A1365.
(50) Bai, Y.; Wang, X.; Zhang, X.; Shu, H.; Yang, X.; Hu, B.; Wei, Q.; Wu, H.; Song, Y. The Kinetics of Li-Ion Deintercalation in the Li-rich Layered $Li_{1.12}[Ni_{0.5}Co_{0.2}Mn_{0.3}]_{0.89}O_2$ Studied by Electrochemical Impedance Spectroscopy and Galvanostatic Intermittent Titration Technique. *Electrochim. Acta* **2013**, *109*, 355−364.
(51) Liu, T.; Garsuch, A.; Chesneau, F.; Lucht, B. L. Surface Phenomena of High Energy $Li(Ni_{1/3}Co_{1/3}Mn_{1/3})O_2$/Graphite Cells at High Temperature and High Cutoff Voltages. *J. Power Sources* **2014**, *269*, 920−926.

DOI: 10.1021/acsami.5b02690
ACS Appl. Mater. Interfaces 2015, 7, 13944−13951

(52) Tasaki, K.; Goldberg, A.; Lian, J. J.; Walker, M.; Timmons, A.; Harris, S. J. Solubility of Lithium Salts Formed on the Lithium-Ion Battery Negative Electrode Surface in Organic Solvents. *J. Electrochem. Soc.* **2009**, *156*, A1019−A1027.
(53) Liu, J.; Manthiram, A. Understanding the Improved Electrochemical Performances of Fe-Substituted 5 V Spinel Cathode $LiMn_{1.5}Ni_{0.5}O_4$. *J. Phys. Chem. C* **2009**, *113*, 15073−15079.

DOI: 10.1021/acsami.5b02690
ACS Appl. Mater. Interfaces 2015, 7, 13944−13951